

Phys. Chem. Res., Vol. 7, No. 4, 715-729, December 2019
DOI: 10.22036/pcr.2019.182691.1621

Why do Bimetallic Clusters have more Chemical Reactivity? Study the V_nNi_m ($2 \leq n + m \leq 6$) Clusters as the Nano Species

A.H. Pakiari*, F. Eshghi and M. Salarhaji

Chemistry Department, Shiraz University, Shiraz, Iran, 7194684795

(Received 22 April 2019, Accepted 29 August 2019)

This article provides some evidence on higher catalytic activity of bimetallic transition metal clusters, with a difference in electronegativity, compared to the monoatomic clusters. In this respect, adsorption of ethylene on bimetallic clusters of vanadium-nickel V_nNi_m ($2 \leq n + m \leq 6$) is investigated. Our results show that hardness has a quite good linear correlation with the non-Lewis MO of V_nNi ($n = 1-5$) cluster ($R^2 = 0.99$). This finding is of particular importance, because, for the first time in literature, it presents an orbital description for hardness. The optimized structure of pure and nickel-doped vanadium clusters and pure and vanadium-doped nickel clusters are studied for up to six atoms. The maximum interaction belongs to nickel substituted alloy, V_nNi ($n = 1-5$). This finding corresponds to the lowest energy gap between HOMO of bimetallic clusters and LUMO of ethylene, according to Fukui equation of reactivity. A successful demonstration has been performed by extrapolation of theoretical results to predict the best mixing of two metals revealing that V_8Ni is the best cluster if it is stable experimentally. We have also demonstrated that the larger bimetallic cluster has more conductivity and reactivity which is the demonstration of nano character.

Keywords: Bimetallic clusters, Global and local reactivity, Bimetallic catalysts, Nickel-vanadium cluster, Softness

INTRODUCTION

It is well-known in literature, both by experiment and theory, that catalytic activity of bimetallic clusters are different (and sometimes better) than that of monoatomic ones due to the mutual influence of added metals [1,2], however, no solid justification has been presented to explain this feature for metals. Bimetallic catalysis has better reactivity, if there are no deactivation conditions, such as (i) poisoning, (ii) fouling, (iii) thermal degradation, (iv) vapor compound formation accompanied by transport, (v) vapor-solid and/or solid-solid reactions and (vi) attrition/crushing.

In the following references, some experimental or theoretical studies for these observations are presented. For example, supported $Co_{4-n}Rh_n$ ($n = 0, 1, 2, \text{ or } 4$) bimetallic clusters used for Fischer-Tropsch synthesis leads to better

performance, because it has better reactivity and selectivity than monometallic species [3]. Adsorption of CO molecule on Au_3Pt clusters was studied by Song *et al.* [4]. The importance of bimetallic clusters can be also seen in Co/Mn [5], Pt/Cu [6], $Cu/V_n^{+/0}$ ($n = 1-5$) [7], Cu/Ni_3 [8], Fe/Cl [9] and Cu/Na or Cu/K [10]. That is why, many research groups focus on alloy systems such as small bimetallic clusters [11,3,12,13]. There is a widely held belief among research groups that bimetallic clusters can be the best models to understand the catalytic reactions [1,14].

The mentioned studies aimed at realizing adsorption strength of small molecules on various bimetallic clusters. However, nothing has been yet published on the experimental and theoretical study of the reactivity of ethylene adsorption on mixed nickel and vanadium clusters. Both nickel, as a late transition metal (TM), and vanadium, as an early TM, show low reactivity toward ethylene adsorption. These observations were the main motivation to

*Corresponding author. E-mail: pakiaariah@gmail.com

realize how the reactivity of vanadium-nickel bimetallic clusters is promoted toward ethylene adsorption in comparison to monoatomic ones. Therefore, the main objective of this research is finding the reasons for higher reactivity of bimetallic clusters in comparison with monoatomic ones. The system of under our investigation is V_nNi_m ($2 \leq n + m \leq 6$) clusters. Density functional theory has been used in this research.

COMPUTATIONAL METHODS

Proposed ground state structures were obtained by applying DFT method using Gaussian 09 program package [15]. The BLYP functional was selected through calibration procedure (Sec 3) because of good performance of BLYP functional for studying the first row of TM clusters [16-18]. Quadruple zeta valence polarized (QZVP) [19] basis set was chosen as an appropriate basis set for our calculations.

The bond dissociation energy (BDE) and adiabatic ionization potential (IP_{ad}) are used for DFT calibration. The required energy for fragmentation of V_nNi_m cluster into $V_{n-1}Ni_m$ or V_nNi_{m-1} and V or Ni atom is called BDE, which is defined by the following equation [Eq. (1)]. BDE of pure clusters is defined as the required energy to fragmentize the M_n cluster into M_{n-1} and M atom (M means metal). The BDE of pure clusters can be computed by [Eq. (2)]:

$$E_{BDE} = E_{V_nNi_m} - ((E_{V_{n-1}Ni_m} \text{ or } E_{V_nNi_{m-1}}) + (E_{V \text{ atom}} \text{ or } E_{Ni \text{ atom}})) \quad (1)$$

$$E_{BDE} = (E_{M \text{ atom}} + E_{M_{n-1}}) - E_{M_n} \quad (2)$$

where $E_{V_nNi_m}$, $E_{V_{n-1}Ni_m}$, $E_{V_nNi_{m-1}}$, $E_{V \text{ atom}}$ and $E_{Ni \text{ atom}}$ are energy of the fragments of bimetallic clusters, vanadium atom, and nickel atom, respectively.

In complexes, binding and interaction energies were calculated. Binding energy is a description of the thermodynamic stability of the system:

$$E_{bind} = E_{complex} - (E_{cluster} + E_{ligand}) \quad (3)$$

where $E_{complex}$, $E_{cluster}$ and E_{ligand} are total energies of complex, pure cluster, and ligand, respectively. As species

encounters with deformation during adsorption process Eq. (3) cannot describe the quality of interactions well. Therefore, interaction energy, E_{int} , is calculated as a function of bond strength [20] by the following equation:

$$E_{int} = E_{bind} - (\Delta E_{metal} + \Delta E_{ligand}) \quad (4)$$

where ΔE_{metal} and ΔE_{ligand} are the deformation energies of metal cluster and ligand, respectively. The difference between the energy of the free molecule in the gas phase geometry and the energy of the isolated and distorted molecule in its complex is called deformation energy. The more negative E_{int} and E_{bind} values are indication of the more stable adsorption.

In interaction of cluster and ligand in their most thermodynamically stable states, change of Gibbs free energy, ΔG , is evaluated by the following equation:

$$\Delta G = \Delta G_{complex} - (\Delta G_{cluster} + \Delta G_{ligand}) \quad (5)$$

where $\Delta G_{complex}$, $\Delta G_{cluster}$ and ΔG_{ligand} are free energies of the complex, cluster, and ligand, respectively.

The natural bond orbital (NBO) [21,22] analysis is an efficient approach for better chemically understanding (electronic point views) of the nature of metal-ligand bonds, through donor/acceptor interactions, depletion of occupancy, and stabilization energies (E_{ij}^2):

$$E_{ij}^2 = \frac{\left| \langle i | \hat{H} | j \rangle \right|^2}{E_j - E_i} \quad (6)$$

where \hat{H} , E_j , E_i and $\langle i | \hat{H} | j \rangle$ are interaction Hamiltonian, orbital energies, and the matrix element, respectively.

Although ionization energy can be obtained as the negative energy of HOMO orbital by Koopmans' theorem, electron affinity (EA) cannot be obtained by LUMO energy, since LUMO is not optimized. However, the better way to calculate IP_{ad} and EA_{ad} with less error is three-point procedure (obtaining total energies of neutral, anion and cation of particular species, called Parr procedure) [23]. Therefore, we calculate IP_{ad} and EA_{ad} through the following equations:

$$IP(Cluster) = E_{tot}(Cluster^+) - E_{tot}(Cluster) \quad (7)$$

$$EA(Cluster) = E_{tot}(Cluster) - E_{tot}(Cluster^-) \quad (8)$$

Then, for evaluation of reactivity index, hardness η is [24],

$$\eta = \frac{(IP - EA)}{2} \quad (9)$$

Global softness as reverse of hardness is calculated by the following equation [25]:

$$s = \frac{1}{\eta} \quad (10)$$

Higher chemical softness is indicative of the higher chemical reactivity. Investigating the local softness can be helpful to predict favorable sites of bimetallic clusters in interaction with ethylene. Finite difference approximation was applied to obtain Fukui function [26,27]:

$$f_k^+ = q_k^{N+1} - q_k^N \quad (11a)$$

$$f_k^- = q_k^N - q_k^{N-1} \quad (11b)$$

$$s_k^+ = f_k^+ \cdot S \quad (12a)$$

$$s_k^- = f_k^- \cdot S \quad (12b)$$

where q_k^N , q_k^{N+1} , and q_k^{N-1} are the electronic populations on selected atom for the N, (N+1) and (N-1) electron systems, respectively. s_k^+ and s_k^- are the local softness for nucleophile and electrophilic attack, respectively. Fukui Equation [26] for interaction between HOMO and LUMO for reactivity is:

$$E_{HOMO,LUMO}^2 = \frac{2 \left| \langle HOMO | \hat{H} | LUMO \rangle \right|^2}{E_{LUMO} - E_{HOMO}} \quad (13)$$

In this equation, HOMO, LUMO, E_{HOMO} , and E_{LUMO} are the highest occupied orbital, lowest unoccupied orbital, HOMO energy, and LUMO energy, respectively.

DFT CALIBRATION

DFT method was preferred in this research, since DFT in the framework of Kohn-Sham is more suitable to calculate TM clusters properties in comparison to *ab initio* methods. DFT methods is not variational, since exact *xc*-functional is not known yet, and all *xc*-functionals are approximate. Therefore, it is necessary to search for appropriate *xc*-functional and basis set for the molecules under our investigation; DFT calibration.

There are many studies for performance of various DFT methods and basis set for TM compounds [16-18]. Truhlar *et al.* [18] research showed that for atomization energies the generalized gradient approximation functional gives more accurate results in comparison to their meta, hybrid, or hybrid meta analogues. They recommended that M06-L and M06 functionals are most appropriate for TM thermochemistry. Truhlar *et al.* [28] showed that PBE functional performance for the series of 30 transition metal elements is most balanced.

Starting point in the study of the V/Ni bimetallic clusters is finding favorable *xc*-functional accompanied by suitable basis set. Calibration must essentially satisfy correct spin multiplicity with least deviation from spin contamination (10^{-2}), successful frequency test and geometry with low percentage of error in comparison to available experimental data, which all guarantee to have a rather correct wave function. There are not any available experimental data for the VNi dimer in the literature [29,30], except spin multiplicity and BDE.

In this research, DFT calibration was carried out with different five recommended *xc*-functionals with QZVP basis set. The results of the dimers calibration are presented in Table 1. The VNi bimetallic dimer has also the lowest spin contamination (10^{-2}) using BLYP/QZVP level of theory calculations, indicating a good agreement with experimental results [29,30]. As a conclusion, BLYP/QZVP is selected for studying the bimetallic clusters, V_nNi_m ($2 \leq n + m \leq 6$), and their interactions with ethylene molecule.

RESULTS AND DISCUSSION

Reactivity of Bimetallic Vanadium-Nickel Clusters

Full studies of pure vanadium and pure nickel clusters

Table 1. Geometries and Energetic Parameters of the Lowest Energy States of VNi, V₂ and Ni₂ Dimers Using Different *xc*-functionals with QZVP Basis Set. The Values in Parentheses are Experimental Data

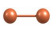

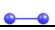


















Clusters	Method	Mul	S ²	N (cm ⁻¹)	BDE (eV)	d (Å)	IP _{ad} (eV)
VNi	BLYP	4 ^a	3.777 (3.750)	269.1	2.89 (2.100) ^b	2.133	5.94
	BP86	4	3.815	264.9	8.82	2.133	3.21
	M06-L	4	3.888	249.2	0.89	2.188	6.26
	TPSS	4	3.828	255.7	2.47	2.139	6.61
	B3LYP	4	3.852	271.5	1.29	2.168	6.42
V ₂	BLYP	3	2.000 (2.00)	622.7 (535.1) ^c	2.974 (2.753) ^c	1.786 (1.774) ^c	6.61
	BP86	3	2.000	637.4	4.265	1.774	6.88
	M06-L	3	2.000	636.3	2.325	1.763	6.11
	TPSS	3	2.000	641.7	2.581	1.777	6.41
	B3LYP	3	2.000	867.8	0.468	1.670	6.10
Ni ₂	BLYP	3	2.000 (2.00)	300.8 (280 ± 20) ^d	2.88	2.147 (2.154) ^d	8.10
	BP86	3	2.000	314.7	7.62	2.122	2.80
	M06-L	3	2.001	317.4	3.84	2.125	7.81
	TPSS	3	2.000	324.6	1.78	2.112	7.87
	B3LYP	3	2.001	330.7	1.19	2.099	8.86

^aRef. [32]. ^bRef. [33]. ^cRef. [31]. ^dRef. [32].

were carried out by Pakiari *et al.* [33,34]. All structures of V_nNi_m (2 ≤ n + m ≤ 6) clusters were optimized without any symmetry constraint, and results including spin multiplicity, IP, EA, HOMO-LUMO gap, percentage of non-Lewis (the explanation of Lewis and non-Lewis is in supplementary at end this manuscript), global hardness, and local softness are collected in Table 2. The basic properties of dimers, such as spin multiplicity, bond length, BDE, frequency and IP_{ad} have been reported in Table 1 in DFT calibration section (Sec 3), where they are in a good agreement with experimental reports [29-32]. Then, NBO analysis for each species is performed that will be discussed in following discussion. The important conclusions obtained from the

results are based upon hardness, non-Lewis portion of electrons, interaction energies and HOMO-LUMO gap. Hardness is also based on IP_{ad} and EA_{ad} obtained by three point procedures ([Eqs. (7) and (8)]). The values of IP_{ad} and EA_{ad} obtained from this procedure are more reliable than Koopmans' theorem, because all species in [Eqs. (7) and (8)] are optimized by DFT methods. The accuracy of IP_{ad} and EA_{ad} values also depends on the accuracy of applied *xc*-functional. Obtaining a correct theoretical value for EA_{ad} is still a challenge in quantum chemistry, as reviewed by Schaefer *et al.* [35]. In order to reduce the error and finding best *xc*-functional, calibration was performed as mentioned before (Sec 3) which was based on diatomic clusters, due to

Table 2. Valance Non-Lewis, Spin Multiplicity, and Global Chemical Reactivity Parameters of V_nNi_m ($2 \leq n + m \leq 6$) Bimetallic Clusters at BLYP/QZVP Level of Theory. ΔE is the HOMO-LUMO Gap Value, and N is the Percentage of Non-Lewis Term

Cluster	Shape	Cluster-type	Mul.	IP _{ad} (eV)	EA (eV)	ΔE (eV)	N	H	S
Dimer		V ₂	3	6.61	0.35	0.5	α : 0.00	3.15	0.32
		VNi	4	6.70	0.71	0.2	α : 0.00	3.00	0.33
		Ni ₂	3	8.10	0.82	0.5	α : 0.00	3.65	0.27
Trimer		V ₃	2	5.94	0.82	0.5	α : 1.81	2.55	0.39
		V ₂ Ni	3	6.01	0.81	0.2	β : 0.87	2.60	0.38
		VNi ₂	4	5.93	0.91	0.3	α : 0.66	2.50	0.40
		Ni ₃	3	6.73	0.94	0.2	β : 1.30	2.90	0.34
Tetramer		V ₄	1	5.28	0.70	0.7	0.85	2.30	0.44
		V ₃ Ni	4	5.07	0.92	0.1	β : 1.85	2.10	0.48
		V ₂ Ni ₂	9	5.35	0.99	0.3	α : 1.63	2.15	0.46
		VNi ₃	6	5.65	1.20	0.3	β : 2.23	2.25	0.44
		Ni ₄	5	5.67	1.30	0.2	α : 0.97	2.20	0.45
Pentamer		V ₅	2	5.10	0.86	0.9	β : 2.70	2.12	0.47
		V ₄ Ni	5	4.19	2.40	0.3	α : 2.02	2.10	0.48
		V ₃ Ni ₂	2	5.33	1.17	0.3	β : 3.03	2.08	0.48
		VNi ₄	2	6.26	1.42	0.3	α : 2.34	3.87	0.26
		Ni ₅	3	6.31	3.87	0.4	β : 1.59	1.22	0.82
Hexamer		V ₆	1	5.17	1.42	0.2	7.30	1.89	0.53
		V ₅ Ni	2	3.70	1.10	0.1	α : 4.17	1.30	0.77
		VNi ₅	2	5.96	1.70	0.2	β : 2.90	2.13	0.47
		Ni ₆	3	6.21	2.03	0.2	β : 1.81	2.09	0.48

availability enough experimental data. Calibration was done for larger clusters, because of the lack of experimental data. Hopefully, this *xc*-functional works for our larger clusters.

This is a disadvantage of DFT that *xc*-functional may change from one species to another, due to lack of the universal *xc*-functional. Fortunately, this *xc*-functional

(BLYP) is suitable for both pure vanadium and pure nickel clusters. Accordingly, the fluctuations in trend of results are expected. However, the calculations show some trends are valuable to be considered.

There are also other sources of error in calculations of IP_{ad} and EA_{ad} which are correlation and relaxation energies explained by Szabo and Ostlund [36]. The error in calculation of HOMO-LUMO energy gap is that HOMO orbital is optimized in DFT procedure, whereas LUMO is not optimized. This gap also depends upon the accuracy of x_c -functional used in our calculations.

It is quite interesting that hardness and non-Lewis of these species, based on the results in Table 2, have a linear relationship ($R^2 = 0.99$), as shown in Fig. 1. Although the results in Table 2 have been generated by quite different theories (Eq. (9) and NBO procedure), this phenomenon is reasonable because non-Lewis is total depletion of occupancies of each molecular orbital in specific species. However, this is important because it is orbital description for hardness. For clarity, non-Lewis will be briefly explained in the supplementary section at end of this manuscript.

It is well-known in chemistry when each molecular orbital is completely filled, it is non-reactive orbital, such as noble gases, and otherwise, it is reactive. When a molecule entirely contains σ -bond, this type of molecule cannot be reactive such as methane (except radical reaction). When a molecule does not have any σ -bond, it still contains some π and δ bonds (especially conjugated π - and δ -bond), lone pair, or has all or some of them. This type of species may have charge transfers within molecular orbitals; donor-acceptor interactions within the molecular orbitals. This phenomenon causes depletion of the molecular orbitals leading to a considerable non-Lewis value (usually between about 2% to 7%). Non-Lewis part is responsible for donation, back donation, and hyper-conjugation in molecule. Our results show that non-Lewis structure reduces hardness, and then the larger reactivity is expected. Therefore, the larger non-Lewis may cause the less hardness and consequently higher reactivity.

The question is which pure monoatomic clusters, nickel or vanadium, is more reactive? Two factors are important for reactivity: HOMO-LUMO gap and hardness (calculated by three-point procedure, mentioned in Computational

Methods, section 2). For pure clusters: nickel clusters Ni_m have lower hardness and smaller HOMO-LUMO gap in comparison with the vanadium clusters (exception: the reverse trend is observed in hardness for dimer, trimer and hexamer of vanadium cluster), shown in Table 2. Therefore, pure nickel cluster is more reactive than pure vanadium cluster. It may be justified by electronegativity of nickel (1.9) compared with vanadium (1.56).

The hardness values of V_nNi_1 are 3.00, 2.60, 2.10, 2.10 and 1.30, for $n = 1$ to 5, respectively, with an average of 2.22, compared to the hardness values of Ni_mV_1 which are 3.00, 2.50, 2.25, 3.87 and 2.13 for $m = 1$ to 5, respectively, with an average of 2.8. Therefore, we can say Ni-doped vanadium clusters with one nickel is more reactive than vanadium-doped nickel clusters. However, when we extrapolate V_nNi_1 hardness, we will obtain minimum hardness of 0.27 for bimetallic nickel-vanadium cluster V_8Ni , Fig. 2, corresponding to 12.4% of nickel in total weight of this bimetallic.

The results show that with increasing the size of bimetallic cluster from dimer to hexamer the IP_{ad} values decrease. We found that among V_nNi clusters, the VNi dimer has the highest IP_{ad} value; the trend is 6.70, 6.01, 5.07, 4.19 and 3.70 eV. The HOMO-LUMO gap values are 0.2, 0.2, 0.1, 0.3 and 0.1 eV for di, tri, tetra, penta and hexatomic V_nNi clusters, respectively, as shown in Table 2. Comparing these gaps with pure metallic gaps of vanadium shows that the reduction is as an average 0.4, and for nickel is 0.1 eV. It means that a bimetallic cluster has a reduction in HOMO-LUMO gap, indicating more conductivity than monoatomic cluster. Therefore, bimetallic clusters behave more nano-character. Quantum mechanically, nickel with electronegativity of 1.90 perturbs valence electrons of vanadium with electronegativity of 1.54, leading more depletion of vanadium orbitals, therefore more non-Lewis, more conductivity, and more reactivity in bimetallic clusters are expected.

Interaction of Vanadium Nickel Bimetallic Cluster with Ethylene

The interactions of V/Ni cluster with ethylene have been studied, and the results of di- σ and π interactions are collected in Tables 3 and 4. Bimetallic TM cluster V_nNi_m generally promotes interaction energy considerably in

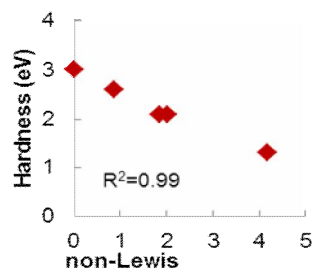


Fig. 1. Linear relationship of global hardness vs. non-Lewis for V_nNi ($n = 1-5$).

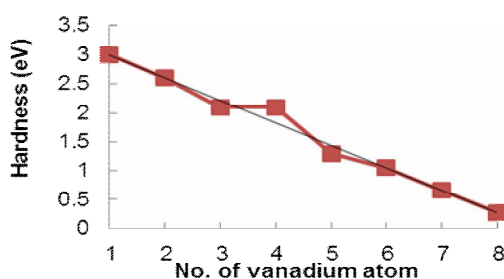


Fig. 2. Extrapolation of hardness vs. number of vanadium atoms in V_nNi ($n = 1-8$) Clusters. The lowest chemical hardness ($\eta = 0.27$ eV) is observed for $n = 8$ (V_8Ni cluster).

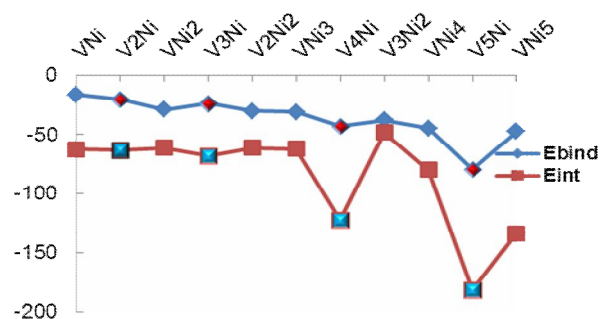


Fig. 3. Trend of E_{bind} and E_{int} of V_nNi_m ($2 \leq n + m \leq 6$) bimetallic clusters; the V_nNi ($n = 1-5$) clusters have the most negative interaction energy.

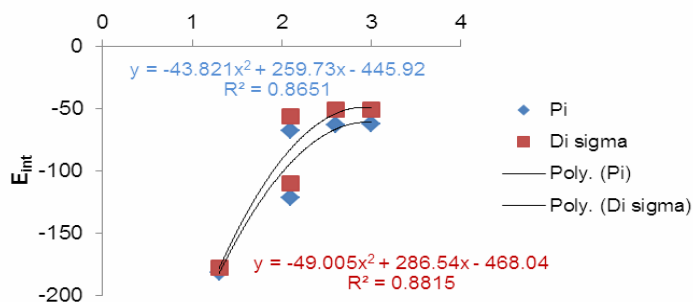
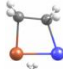
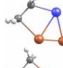
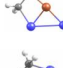
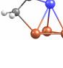
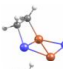
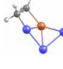

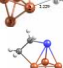
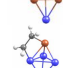

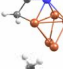


Fig. 4. Quadratic correlation for hardness against interaction energy for V_nNi ($n = 1-5$).

Table 3. Interaction of the most Stable V_nNi_m ($2 \leq n + m \leq 6$) Clusters with Ethylene Molecule, Gibbs Free Energy, Binding (Adsorption) Energy, and Interaction Energy in di- σ Mode (in kcal mol⁻¹)

Cluster	di- σ	Mul.	E_{bind}	$\Delta E_{\text{bimetal}}$	$\Delta E_{\text{ethylene}}$	E_{int}	non-Lewis	Hardness	ΔG
VNi		4	-21.0	5.5	24.3	-50.8	0.0	3.0	-11.5
V ₂ Ni		3	-10.4	10.5	30.3	-51.2	0.87	2.60	+0.2
VNi ₂		2	-27.6	3.9	26.1	-57.6	0.66	2.50	-16.2
V ₃ Ni		2	-23.5	8.3	24.9	-56.7	1.85	2.10	-11.4
V ₂ Ni ₂		5	-30.5	21.2	11.3	-63.0	1.63	2.15	-19.7
VNi ₃		4	-30.9	28.0	3.3	-62.2	2.23	2.25	-20.8
V ₄ Ni		3	-33.4	3.6	76.0	-110.4	2.02	2.10	-22.4
V ₃ Ni ₂		2	-13.5	8.5	24.8	-46.8	3.34	2.05	-2.2
VNi ₄		2	-44.7	0.9	9.7	-55.3	2.34	3.87	-34.4
V ₅ Ni		2	-74.9	34.4	68.6	-177.9	4.17	1.31	-62.3
VNi ₅		2	-50.7	0.4	47.2	-98.3	2.90	2.13	-39.3

Interaction energies (in kcal mol⁻¹) of pure clusters with ethylene in di- σ mode, V₂: -38.9, V₃: -41.2, V₄: -52.9, V₅: -74.6, V₆: -96.1 and Ni₂: -47.3, Ni₃: -48.8, Ni₄: -36.5, Ni₅: -67.8, Ni₆: -86.8.

comparison to monoatomic TM cluster V_n or Ni_m clusters either for di- σ or π -orientations. As shown in Table 5, these promotions are as average of 39.04% for di- σ in comparison with pure vanadium cluster, and 47.10% as an average in comparison with pure nickel cluster. Tables 5 and 7 also clearly show that interaction energy is directly related to the local softness: when the local softness is high, the interaction energy is high, and the longer bond length is expected, or vice versa. Table 6 shows that the promotion of interaction energies in π -orientation is as average of 42.84% in comparison with pure vanadium cluster, and 33.12% in comparison with pure nickel cluster. For instance, in Tables 5 and 7, when local softness for π Ni in VNi is 0.83 eV, the corresponding E_{int} is -62.6 kcal mol⁻¹, and bond length is

1.987 a.u., whereas for π Ni in V₅Ni with a softness of 4.35 eV, the E_{int} is -181.8 kcal mol⁻¹ and bond length is 2.061 a.u. The best interaction energy was obtained for π mode as shown in Tables 3 and 4 and Fig. 3. More importantly, for π mode, interaction energy from nickel site is more negative than that from vanadium site (Table 4) and the most negative interaction energies in the π mode are obtained when one atom in vanadium cluster is substituted by the nickel atom (V_nNi), as shown in Table 6, and Fig. 3. The extrapolation of these results reveals that substitution of 10% of nickel atom in vanadium catalysis caused a maximum hardness, as shown in Fig. 2. This conclusion can be checked with theory of Frontier Orbital by Fukui [26] [Eq. (13)] expressing that the best interaction energy can be

Table 4. Interaction of the most Stable V_nNi_m ($2 \leq n + m \leq 6$) Clusters with Ethylene Molecule, Gibbs Free Energy, Binding (Adsorption) Energy, and Interaction Energy in π Mode*

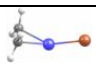


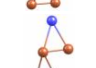
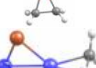

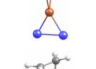
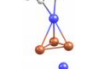

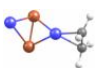
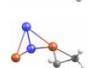
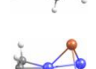
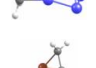
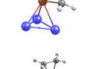
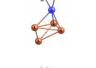
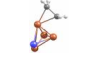

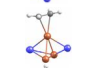
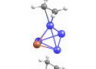
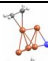

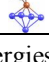
Cluster	Site	π mode	Mul	E_{bind}	$\Delta E_{\text{bimetal}}$	$\Delta E_{\text{ethylene}}$	E_{int}	non-Lewis	Softness (local)	ΔG
VNi	Ni		4	-16.4	19.2	27.0	-62.6	0.0	0.83	-9.3
VNi	V		4	-18.8	3.9	28.2	-50.9	0.0	0.56	-9.5
V ₂ Ni	Ni		3	-20.2	20.5	22.6	-63.3	0.87	1.35	-10.6
V ₂ Ni	V		1	-23.7	1.7	31.1	-56.5	0.87	1.08	-11.8
VNi ₂	Ni		4	-28.7	0.9	17.3	-46.9	0.66	2.22	-14.4
VNi ₂	V		2	-25.2	0.9	19.4	-45.5	0.66	1.33	-18.3
V ₃ Ni	Ni		2	-23.6	15.8	28.6	-68.0	1.85	2.94	-12.5
V ₃ Ni	V		4	-56.6	3.5	6.7	-66.8	1.85	1.35	-16.5
V ₂ Ni ₂	Ni		5	-29.9	6.2	25.3	-61.4	1.63	3.12	-19.4
V ₂ Ni ₂	V		5	-38.3	4.8	13.2	-56.3	1.63	1.32	-29.8
VNi ₃	Ni		4	-29.6	4.3	27.8	-61.7	2.23	2.13	-19.7
VNi ₃	V		6	-30.9	0.6	28.5	-60.0	2.23	1.33	-20.0
V ₄ Ni	Ni		3	-42.7	3.6	76.0	-122.3	2.02	4.76	-32.1
V ₄ Ni	V		3	-60.2	6.1	26.6	-92.9	2.02	2.08	-16.8
V ₃ Ni ₂	Ni		2	-37.9	0.1	10.3	-48.3	3.34	1.67	-26.6
V ₃ Ni ₂	V		2	-3.2	8.3	25.5	-37.0	3.34	1.67	-12.4
VNi ₄	Ni		2	-59.4	11.4	9.1	-79.9	2.34	0.98	-48.8
VNi ₄	V		10	-4.9	4.1	3.0	-12.0	2.34	0.75	+4.7
V5Ni	Ni		2	-79.4	33.3	69.1	-181.8	4.17	4.35	-69.0

Table 4. Continued

V ₅ Ni	V		2	-44.9	27.8	68.6	-141.3	4.17	3.45	-33.3
VNi ₅	Ni		2	-47.6	0.7	85.5	-133.8	2.90	2.56	-37.2
VNi ₅	V		2	-50.7	1.0	78.5	-130.2	2.90	1.89	-39.3

*Interaction energies (in kcal mol⁻¹) of pure clusters with ethylene in the π mode, V₂: -23.7, V₃: -38.5, V₄: -55.2, V₅: -89.4, V₆: -110.7, Ni₂: -49.9, Ni₃: -45.8, Ni₄: -57.6, Ni₅: -99.5, Ni₆: -112.7.

Table 5. Comparing the Interaction Energies (in kcal mol⁻¹) in the di- σ Mode of Bimetallic Clusters with Mono Metallic Clusters

Clusters	E _{int}	Clusters	s _{Ni}	E _{int}	%a	Clusters	s _V	E _{int.}	%b
VNi	-50.8	Ni ₂	0.55	-47.3	7.4	V ₂	0.63	-38.9	30.6
V ₂ Ni	-51.2	Ni ₃	1.21	-48.8	5.0	V ₃	1.39	-41.2	24.3
V ₃ Ni	-56.7	Ni ₄	2.86	-36.5	55.3	V ₄	1.89	-52.9	7.2
V ₄ Ni	-110.4	Ni ₅	3.05	-67.8	62.8	V ₅	3.03	-74.6	48.0
V ₅ Ni	-177.9	Ni ₆	3.47	-86.8	105.0	V ₆	3.57	-96.1	85.1

a and b are promotion of interaction energies with respect to Ni and V clusters, respectively.

Table 6. Comparing the Interaction Energies (in kcal mol⁻¹) in the π Mode of BTMCs with those in Mono Metallic Clusters

Cluster	π -Ni ^a	E _{int}	%a	π -V ^a	E _{int.}	%b	Cluster	s*	E _{int}	clusters	s*	E _{int.}
VNi	0.83	-62.6	25.4	0.56	-50.9	114.8	Ni ₂	0.55	-49.9	V ₂	0.63	-23.7
V ₂ Ni	1.35	-63.3	38.2	1.08	-56.5	46.8	Ni ₃	1.21	-45.8	V ₃	1.39	-38.5
V ₃ Ni	2.94	-68.0	18.1	1.35	-66.8	21.0	Ni ₄	2.86	-57.6	V ₄	1.89	-55.2
V ₄ Ni	4.76	-122.0	22.6	2.08	-92.9	4.0	Ni ₅	3.05	-99.5	V ₅	3.03	-89.4
V ₅ Ni	4.35	-181.8	61.3	3.45	-141.3	27.6	Ni ₆	3.47	-112.7	V ₆	3.57	-110.7

a and b are promotion of interaction energies with respect to Ni clusters and V clusters, respectively. *means local softness (eV).

obtained in bimolecular interaction by second order perturbation, when energy gap between HOMO of cluster and LUMO of ethylene is the smallest, as shown in Table 8.

However, interaction energy has a quadratic relationship with hardness, as shown in Fig. 4.

Our results indicate that S has an ascending trend with

Table 7. Correlation of Bond lengths and Local Softness Values in the V_nNi ($n = 1-5$) Clusters

Clusters	Ni*	d_{Ni-C}	V*	d_{V-C}
VNi	0.83	1.987	0.56	2.068
V_2Ni	1.35	2.042	1.08	2.271
V_3Ni	2.94	1.974	1.35	2.188
V_4Ni	4.76	2.046	2.08	2.230
V_5Ni	4.35	2.061	3.45	2.289

d means distance, *means local softness (eV).

Table 8. V_nNi_m -HOMO and C_2H_4 -LUMO Gaps and their Corresponding Energies (in eV)

Cluster	HOMO Cluster	LUMO C_2H_4	Energy gap
V_2	-3.6	-1.8 ^a	1.8
VNi	-3.2	-1.8	1.4
Ni_2	-4.1	-1.8	2.3
V_3	-3.1	-1.8	1.3
V_2Ni	-3.4	-1.8	1.6
VNi_2	-3.3	-1.8	1.5
Ni_3	-3.4	-1.8	1.6
V_4	-3.1	-1.8	1.3
V_3Ni	-3.0	-1.8	1.2
V_2Ni_2	-3.2	-1.8	1.4
VNi_3	-3.4	-1.8	1.6
Ni_4	-3.5	-1.8	1.7
V_5	-3.4	-1.8	1.6
V_4Ni	-3.3	-1.8	1.5
V_3Ni_2	-3.2	-1.8	1.4
VNi_4	-3.7	-1.8	1.9
Ni_5	-3.8	-1.8	2.0
V_6	-3.5	-1.8	1.7
V_5Ni	-3.3	-1.8	1.5
VNi_5	-3.9	-1.8	2.1
Ni_6	-4.1	-1.8	2.3

^aRef. [37]. (1.78 ± 0.05 eV).

the size of V_n ($n = 2-6$) clusters, S: $V_6 > V_5 > V_4 > V_3 > V_2$, while for Ni_m ($m = 2-6$) the trend is, $Ni_5 > Ni_6 > Ni_4 > Ni_3 > Ni_2$, and there is not organized trend in V_nNi_m ($2 \leq n + m \leq 6$) bimetallic clusters, as shown in Table 2. Doping the Ni atoms in pure vanadium clusters leads to increasing chemical softness values and consequently higher reactivity in comparison with pure nickel or vanadium cluster.

CONCLUSIONS

This study provides some evidence on higher reactivity of bimetallic clusters, V_nNi_m ($2 \leq n + m \leq 6$), compared to monoatomics, due to the considerable term of non-Lewis in electronic structure of bimetallics. Hardness of these species has a good correlation with non-Lewis part of electronic structure of our clusters, ($R^2 = 0.99$). Additionally, hardness has also a rather good correlation with interaction energy (second-degree polynomial $R^2 = 0.88$). The extrapolation of the results V_nNi ($n = 1-8$) shows that the most reactive species is V_8Ni . The results show that the larger bimetallic cluster has more conductivity and reactivity than monoatomic cluster, which is indicative of a nano character.

SUPPLEMENTARY

Non-Lewis results are obtained by NBO analysis, based on natural orbital introduced by Lowdin [38]. All electrons in molecule by NBO procedure are divided into mainly two categories; Lewis and non-Lewis. Lewis part is the classical definition of valance theory of electronic structure of molecule introduced by Lewis, and is more or less between 94% to 100% of total electrons in our species, and depends on specific molecule. Some molecules have 100% of electrons as Lewis such as methane. Lewis part is also called localized orbitals. Small portion of electronic structure of molecule, which is delocalized part and more or less is 6%, is called non-Lewis of electronic structure of molecule. Non-Lewis part is actually antibonding, and responsible for charge transfer and donor-acceptor of electrons, back bonding and hyperconjugation giving rise the depletion of occupancies of some molecular orbitals.

REFERENCES

- [1] Ferrando, R.; Jellinek, J.; Johnston, R. L., Nanoalloys: From theory to applications of alloy clusters and nanoparticles. *Chem. Rev.* **2008**, *108*, 845-910, DOI: <http://doi.org/10.1021/cr040090g>.
- [2] Johnston, R. L.; Ferrando, R., *Preface Faraday Discuss.* **2008**, *138*, 9-10, DOI: <http://doi.org/10.1039/B717388C>.
- [3] Kiviaho, J., Fischer-Tropsch Synthesis Catalysed by Cobalt-rhodium and Cobalt-ruthenium Carbonyl Clusters on Silica. Technical Research Centre of Finland, 1996.
- [4] Song, C.; Ge, Q.; Wang, L., DFT studies of Pt/Au bimetallic clusters and their interactions with the CO molecule. *J. Phys. Chem. B.* **2005**, *109*, 22341-22350, DOI: <http://doi.org/10.1021/jp0546709>.
- [5] Du, J.; Wu, G.; Wang, J., Density functional theory study of the interaction of carbon monoxide with bimetallic Co-Mn clusters. *J. Phys. Chem. A.* **2010**, *114*, 10508-10514, DOI: <http://doi.org/10.1021/jp106321s>.
- [6] Avdeev, V. I.; Kovalchuk, V. I.; Zhidomirov, G. M.; d'Itri, J. L., Ethylene adsorption on the Pt-Cu bimetallic catalysts. Density functional theory cluster study. *Surf. Sci.* **2005**, *583*, 46-59, DOI: <https://doi.org/10.1016/j.susc.2005.03.021>.
- [7] Yuan, J.; Li, G.; Yang, B.; Zhang, J.; Li, Z.; Chen, H., Selective adsorption of ethylene on bimetallic $CuVn+0$ ($n = 1-5$) clusters: A theoretical study. *Comput. Mater. Sci.* **2016**, *111* 489-496, DOI: <https://doi.org/10.1016/j.commatsci.2015.09.064>.
- [8] Derosa, P. A.; Seminario, J. M.; Balbuena, P. B., Properties of small bimetallic Ni-Cu clusters. *J. Phys. Chem. A.* **2001**, *105*, 7917-7925, DOI: <http://doi.org/10.1021/jp0104637>.
- [9] Pahlavan, F.; Pakiari, A. H., DFT study of the chlorine promotion effect on the ethylene adsorption over iron clusters. *J. Mol. Graphics Modell.* **2016**, 6658-66, DOI: <https://doi.org/10.1016/j.jmglm.2016.03.009>.
- [10] Shariati, S.; Pakiari, A. H., Role of alkali metal additives on adsorption of CO on small copper clusters [Cu_nAM_m ($m + n = 7, m < n$)]: A DFT study

- Comput. Theor. Chem.* **2017**, 109992-101, DOI: <https://doi.org/10.1016/j.comptc.2016.11.015>.
- [11] Félix-Navarro, R.; Beltrán-Gastélum, M.; Salazar-Gastélum, M.; Silva-Carrillo, C.; Reynoso-Soto, E.; Pérez-Sicairos, S.; Lin, S.; Paraguay-Delgado, F.; Alonso-Núñez, G., Pt-Pd bimetallic nanoparticles on MWCNTs: catalyst for hydrogen peroxide electrosynthesis. *J. Nanopart. Res.* **2013**, *15*, 1802, DOI: <https://doi.org/10.1007/s11051-013-1802-3>.
- [12] Li, W.; Liu, C.; Abroshan, H.; Ge, Q.; Yang, X.; Xu, H.; Li, G., Catalytic CO oxidation using bimetallic MxAu_{25-x} clusters: A combined experimental and computational study on doping effects. *J. Phys. Chem. C.* **2016**, *120*, 10261-10267, DOI: <http://doi.org/10.1021/acs.jpcc.6b00793>.
- [13] Garcia, T.; Murillo, R.; Agouram, S.; Dejoz, A.; Lazaro, M. J.; Torrente-Murciano, L.; Solsona, B., Highly dispersed encapsulated AuPd nanoparticles on ordered mesoporous carbons for the direct synthesis of H₂O₂ from molecular oxygen and hydrogen. *Chem. Commun.* **2012**, *48*, 5316-5318, DOI: <http://doi.org/10.1039/C2CC14667C>.
- [14] Freund, H. J.; Libuda, J.; Bäumer, M.; Risse, T.; Carlsson, A., Cluster, facets and edges: Site-dependent selective chemistry on model catalysts. *Chem. Rec.* **2003**, *3*, 181-201, DOI: <https://doi.org/10.1002/tcr.10060>.
- [15] Frisch, M. J.; Trucks, G. W.; Schlegel, H. B.; Scuseria, G. E.; Robb, M. A.; Cheeseman, J. R.; Scalmani, G.; Barone, V.; Mennucci, B.; Petersson, G. A.; Nakatsuji, H.; Caricato, M.; Li, X.; Hratchian, H. P.; Izmaylov, A. F.; Bloino, J.; Zheng, G.; Sonnenberg, J. L.; Hada, M.; Ehara, M.; Toyota, K.; Fukuda, R.; Hasegawa, J.; Ishida, M.; Nakajima, T.; Honda, Y.; Kitao, O.; Nakai, H.; Vreven, T.; Montgomery, J. A.; Peralta, J. E.; Ogliaro, F.; Bearpark, M.; Heyd, J. J.; Brothers, E.; Kudin, K. N.; Staroverov, V. N.; Kobayashi, R.; Normand, J.; Raghavachari, K.; Rendell, A.; Burant, J. C.; Iyengar, S. S.; Tomasi, J.; Cossi, M.; Rega, N.; Millam, J. M.; Klene, M.; Knox, J. E.; Cross, J. B.; Bakken, V.; Adamo, C.; Jaramillo, J.; Gomperts, R.; Stratmann, R. E.; Yazyev, O.; Austin, A. J.; Cammi, R.; Pomelli, C.; Ochterski, J. W.; Martin, R. L.; Morokuma, K.; Zakrzewski, V. G.; Voth, G. A.; Salvador, P.; Dannenberg, J. J.; Dapprich, S.; Daniels, A. D.; Farkas, Foresman, J. B.; Ortiz, J. V.; Cioslowski, J.; Fox, D. J., (2009) Gaussian 09, Revision A.01. Wallingford CT.
- [16] Furche, F.; Perdew, J. P., The performance of semilocal and hybrid density functionals in 3d transition-metal chemistry. *J. Chem. Phys.* **2006**, *124*, 044103, DOI: <https://doi.org/10.1063/1.2162161>.
- [17] Zhao, Y.; Truhlar, D. G., Comparative assessment of density functional methods for 3d transition-metal chemistry. *J. Chem. Phys.* **2006**, *124*, 224105, DOI: <http://doi.org/10.1063/1.2202732>.
- [18] Cramer, C. J.; Truhlar, D. G., Density functional theory for transition metals and transition metal chemistry. *PCCP.* **2009**, *11*, 10757-10816, DOI: <http://doi.org/10.1039/B907148B>.
- [19] Weigend, F.; Furche, F.; Ahlrichs, R., Gaussian basis sets of quadruple zeta valence quality for atoms H-Kr. *J. Chem. Phys.* **2003**, *119*, 12753-12762, DOI: <https://doi.org/10.1063/1.1627293>.
- [20] Russo, N.; Salahub, D., Metal-Ligand Interactions in Chemistry, Physics and Biology, Vol. 546 of Nato Science Series. Series C: Mathematical and Physical Sciences. Kluwer Academic Publishers: Dordrecht, 2000.
- [21] Reed, A. E.; Weinstock, R. B.; Weinhold, F., Natural population analysis. *J. Chem. Phys.* **1985**, *83*, 735-746, DOI: <https://doi.org/10.1063/1.449486>.
- [22] Reed, A. E.; Curtiss, L. A.; Weinhold, F., Intermolecular interactions from a natural bond orbital, donor-acceptor viewpoint. *Chem. Rev.* **1988**, *88*, 899-926, DOI: <http://doi.org/10.1021/cr00088a005>.
- [23] Parr, R. G.; Yang, W., Density-Functional Theory of Atoms and Molecules. Oxford University Press, USA, 1994.
- [24] Parr R. G.; Pearson R. G., Absolute hardness: companion parameter to absolute electronegativity. *J. Am. Chem. Soc.* **1983**, *105*, 7512-7516, DOI: <http://doi.org/10.1021/ja00364a005>
- [25] Yang, W.; Parr, R. G., Hardness, softness, and the Fukui function in the electronic theory of metals and catalysis. *Proc. Natl. Acad. Sci.* **1985**, *82*, 6723-6726,

- DOI: <https://doi.org/10.1073/pnas.82.20.6723>.
- [26] Fukui, K.; Fujimoto, H., *Frontier Orbitals and Reaction Paths: Selected Papers of Kenichi Fukui*. World Scientific, 1997.
- [27] Yang, W.; Mortier, W. J., The use of global and local molecular parameters for the analysis of the gas-phase basicity of amines. *J. Am. Chem. Soc.* **1986**, *108*, 5708-5711, DOI: <http://doi.org/10.1021/ja00279a008>.
- [28] Janthon, P.; Luo, S.; Kozlov, S. M.; Vines, F.; Limtrakul, J.; Truhlar, D. G.; Illas, F., Bulk properties of transition metals: a challenge for the design of universal density functionals. *J. Chem. Theory Comput.* **2014**, *10*, 3832-3839, DOI: <http://doi.org/10.1021/ct500532v>.
- [29] Spain, E. M.; Morse, M. D., Bond strengths of transition metal diatomics: VN_i and V₂. *Int. J. Mass Spectrom. Ion Processes.* **1990**, 102183-197, DOI: [https://doi.org/10.1016/0168-1176\(90\)80059-C](https://doi.org/10.1016/0168-1176(90)80059-C).
- [30] Spain, E. M.; Morse, M. D., Bond strengths of transition-metal dimers: titanium-vanadium (TiV), vanadium dimer, titanium-cobalt (TiCo), and vanadium-nickel (VN_i). *J. Phys. Chem.* **1992**, *96*, 2479-2486, DOI: <http://doi.org/10.1021/j100185a018>.
- [31] Langridge-Smith, P. R.; Morse, M. D.; Hansen, G.; Smalley, R.; Merer, A. J., The bond length and electronic structure of V₂. *J. Chem. Phys.* **1984**, *80*, 593-600, DOI: <https://doi.org/10.1063/1.446769>.
- [32] De Vore, T. C.; Ewing, A.; Franzen, H. F.; Calder, V., The visible absorption spectra of Mn₂, Fe₂, and Ni₂ in argon matrices. *Chem. Phys. Lett.* **1975**, *35*, 78-81, DOI: [https://doi.org/10.1016/0009-2614\(75\)85592-8](https://doi.org/10.1016/0009-2614(75)85592-8).
- [33] Pakiari, A. H.; Pahlavan, F., The electronic structures of small N_n (n = 2-4) clusters and their interactions with ethylene and triplet oxygen: A theoretical study. *Chem. Phys. Chem.* **2014**, *15*, 4055-4066, DOI: <https://doi.org/10.1002/cphc.201402467>.
- [34] Pakiari, A. H.; Eshghi, F., Geometric and electronic structures of vanadium sub-nano clusters, V_n (n = 2-5), and their adsorption complexes with CO and O₂ ligands: A DFT-NBO study. *Phys. Chem. Res.* **2017**, *5*, 601-615, DOI: <https://dx.doi.org/10.22036/pcr.2017.80624.1364>.
- [35] Rienstra-Kiracofe, J. C.; Tschumper, G. S.; Schaefer, H. F.; Nandi, S.; Ellison, G. B., Atomic and molecular electron affinities: photoelectron experiments and theoretical computations. *Chem. Rev.* **2002**, *102*, 231-282, DOI: <http://doi.org/10.1021/cr990044u>.
- [36] Szabo, A.; Ostlund, N. S., *Modern Quantum Chemistry: Introduction to Advanced Electronic Structure Theory*. Dover Publications, 1996.
- [37] Chiu, N.; Burrow, P.; Jordan, K., Temporary anions of the fluoroethylenes. *Chem. Phys. Lett.* **1979**, *68*, 121-126, DOI: [https://doi.org/10.1016/0009-2614\(79\)80082-2](https://doi.org/10.1016/0009-2614(79)80082-2).
- [38] Löwdin, P. -O., Quantum theory of many-particle systems. I. Physical interpretations by means of density matrices, natural spin-orbitals, and convergence problems in the method of configurational interaction. *Phys. Rev.* **1955**, *97*, 1474-1489, DOI: <https://doi.org/10.1103/PhysRev.97.1474>.
- [39] Naito, S.; Hasebe, T.; Miyao, T., Remarkable addition effect of In and Ga in the NO-CO reaction over Pd/SiO₂. *Chem. Lett.* **1998**, *27*, 1119-1120, DOI: <https://doi.org/10.1246/cl.1998.1119>.
- [40] Cordoba, G.; Fierro, J.; Lopez-Gaona, A.; Martin, N.; Viniegra, M., Probing Ru- PdSiO₂ catalysts by gas phase o-xylene hydrogenation. *J. Mol. Catal. A: Chem.* **1995**, *96*, 155-161, DOI: [https://doi.org/10.1016/1381-1169\(94\)00041-7](https://doi.org/10.1016/1381-1169(94)00041-7).
- [41] Recchia, S.; Dossi, C.; Poli, N.; Fusi, A.; Sordelli, L.; Psaro, R., Outstanding performances of magnesia-supported platinum-tin catalysts for citral selective hydrogenation. *J. Catal.* **1999**, *184*, 1-4, DOI: <https://doi.org/10.1006/jcat.1999.2485>.
- [42] Adams, R. D.; Barnard, T. S., Does a metal to metal "ligand" effect influence the catalytic activity of bimetallic cluster complexes? Synthesis and catalytic activity of Pt₃Ru₆(CO)₁₉(SMe₂)(μ₃-PhC₂Ph)(μ₃-H)(μ-H). *Organometallics.* **1998**, *17*, 2885-2890, DOI: <http://doi.org/10.1021/om980208h>.
- [43] Zhang, S.; Shan, J. -J.; Zhu, Y.; Frenkel, A. I.; Patlolla, A.; Huang, W.; Yoon, S. J.; Wang, L.; Yoshida, H.; Takeda, S., WGS catalysis and *in situ* studies of CoO_{1-x}, PtCo_n/Co₃O₄, and Pt_mCo_n/CoO_{1-x} nanorod catalysts. *J. Am. Chem. Soc.* **2013**, *135*, 8283-8293, DOI: <http://doi.org/10.1021/ja401967y>.

- [44] Nguyen, L.; Zhang, S.; Wang, L.; Li, Y.; Yoshida, H.; Patlolla, A.; Takeda, S.; Frenkel, A. I.; Tao, F., Reduction of nitric oxide with hydrogen on Catalysts of singly dispersed bimetallic sites Pt₁Co_n and Pd₁Co_n. *ACS Catal.* **2016**, *6*, 840-850, DOI: <http://doi.org/10.1021/acscatal.5b00842>.
- [45] Boucher, M. B.; Zugic, B.; Cladaras, G.; Kammert, J.; Marcinkowski, M. D.; Lawton, T. J., Sykes, ECH., flytzani-stephanopoulos, M., Single atom alloy surface analogs in Pd_{0.18}Cu₁₅ nanoparticles for selective hydrogenation reactions. *PCCP.* **2013**, *15*, 12187-12196, DOI: <http://doi.org/10.1039/C3CP51538A>.
- [46] Miura, H.; Endo, K.; Ogawa, R.; Shishido, T., Supported palladium-gold alloy catalysts for efficient and selective hydrosilylation under mild conditions with isolated single palladium atoms in alloy nanoparticles as the main active site. *ACS Catal.* **2017**, *7*, 1543-1553, DOI: <http://doi.org/10.1021/acscatal.6b02767>.
- [47] Zhang, L.; Wang, A.; Miller, J. T.; Liu, X.; Yang, X.; Wang, W.; Li, L.; Huang, Y.; Mou, C. -Y.; Zhang, T., Efficient and durable Au alloyed Pd single-atom catalyst for the Ullmann reaction of aryl chlorides in water. *ACS Catal.* **2014**, *4*, 1546-1553, DOI: <http://doi.org/10.1021/cs500071c>.